EARTH SURFACE PROCESSES AND LANDFORMS
Earth Surf. Process. Landforms (2016)

Published online in Wiley Online Library
(wileyonlinelibrary.com) DOI: 10.1002/esp.4044

Using UAV acquired photography and structure from motion techniques for studying glacier landforms: application to the glacial flutes at Isfallsglaciären

Jeremy C. Ely,[1]* Conor Graham,[2] Iestyn D. Barr,[2] Brice R. Rea,[3] Matteo Spagnolo[3] and Jeff Evans[4]
[1] Department of Geography, The University of Sheffield, Sheffield, S10 2TN, UK
[2] School of Geography, Archaeology and Palaeoecology, Queen's University Belfast, Belfast, BT7 1NN, UK
[3] School of Geosciences, University of Aberdeen, Aberdeen, AB24 3UF, UK
[4] Department of Geography, Loughborough University, Loughborough, LE11 3TU, UK

Received 21 March 2016; Revised 22 August 2016; Accepted 1 September 2016

*Correspondence to: Jeremy Ely, Department of Geography, The University of Sheffield, Sheffield, S10 2TN, UK. E-mail: j.ely@sheffield.ac.uk

ESPL
Earth Surface Processes and Landforms

ABSTRACT: Glacier and ice sheet retreat exposes freshly deglaciated terrain which often contains small-scale fragile geomorphological features which could provide insight into subglacial or submarginal processes. Subaerial exposure results in potentially rapid landscape modification or even disappearance of the minor-relief landforms as wind, weather, water and vegetation impact on the newly exposed surface. Ongoing retreat of many ice masses means there is a growing opportunity to obtain high resolution geospatial data from glacier forelands to aid in the understanding of recent subglacial and submarginal processes. Here we used an unmanned aerial vehicle to capture close-range aerial photography of the foreland of Isfallsglaciären, a small polythermal glacier situated in Swedish Lapland. An orthophoto and a digital elevation model with ~2 cm horizontal resolution were created from this photography using structure from motion software. These geospatial data was used to create a geomorphological map of the foreland, documenting moraines, fans, channels and flutes. The unprecedented resolution of the data enabled us to derive morphological metrics (length, width and relief) of the smallest flutes, which is not possible with other data products normally used for glacial landform metrics mapping. The map and flute metrics compare well with previous studies, highlighting the potential of this technique for rapidly documenting glacier foreland geomorphology at an unprecedented scale and resolution. The vast majority of flutes were found to have an associated stoss-side boulder, with the remainder having a likely explanation for boulder absence (burial or erosion). Furthermore, the size of this boulder was found to strongly correlate with the width and relief of the lee-side flute. This is consistent with the lee-side cavity infill model of flute formation. Whether this model is applicable to all flutes, or multiple mechanisms are required, awaits further study. © 2016 The Authors. Earth Surface Processes and Landforms published by John Wiley & Sons Ltd.

KEYWORDS: UAV; structure from motion; DEM; glacial flutes; glacial geomorphology

Introduction

Elucidating the processes which operate at the ice–bed interface is key to understanding how an ice mass moves over its bed (Weertman, 1957; Iverson and Semmens, 1995; Kjær *et al.*, 2006). The recession of ice reveals landforms, imprinted on the landscape, from which we can make inferences regarding the subglacial environment and palaeo-glaciological conditions. The identification, mapping and interpretation of these landforms is a cornerstone of palaeo-glaciological reconstruction (Kleman and Borgström, 1996; Stokes *et al.*, 2015), enabling the identification of past surge events (Evans and Rea, 1999; Rea and Evans, 2011), palaeo ice streams (Stokes and Clark, 1999), ice flow direction changes (Clark, 1993) and past ice extent (Bradwell *et al.*, 2008; Barr and Clark, 2009).

The landforms created by ice sheets, including subglacial bedforms (Clark *et al.*, 2009; Spagnolo *et al.*, 2014), eskers (Storrar *et al.*, 2013) and large moraines (Barr and Clark, 2009), are visible on digital elevation model (DEM) products and satellite imagery, which can have a near global coverage (e.g., the Landsat archive, and ASTER GDEM). However, many of the landforms found on glacier forelands (i.e. in recently deglaciated areas) are often too small to be mapped from these sources. Examples include crevasse squeeze ridges (Bennett *et al.*, 1996; Rea and Evans, 2011), eskers (Evans *et al.*, 2010; Storrar *et al.*, 2015) and glacial flutes (Gordon *et al.*, 1992; Hart, 1995; Kjær *et al.*, 2006). Deglaciation exposes forelands to subaerial modification (Mattson and Gardner, 1991; Etzelmüller *et al.*, 2000; Lukas *et al.*, 2005; Irvine-Fynn *et al.*, 2011; Kirkbride and Winkler, 2012) and when the landforms are relatively small, as is the case for flutes, this

may rapidly modify, mask and/or erase their presence (Rose, 1991). Physical mapping using ground-based survey is time consuming in these terrains and can be logistically challenging. However, rapidly acquired, high resolution imagery and DEMs could provide robust and large datasets recording these fragile and transient landforms.

Conventional aerial photography can provide sufficient detail to map the distribution of relatively small-scale features on a glacier foreland (Evans *et al.*, 2007; Jónsson *et al.*, 2014). Recently, high-resolution (< 0.5 m) satellite imagery has also been used to study glacier foreland geomorphology (Chandler *et al.*, 2015; Evans *et al.*, 2016a). However, for the smallest (< 2 m) of glacial landforms, the resolution is still often insufficient to accurately determine all relevant size and shape metrics, key constraints upon their formation (Clark *et al.*, 2009; Spagnolo *et al.*, 2014; Storrar *et al.*, 2014; Ely *et al.*, 2016). Moreover, high-resolution, commercial aerial photography (and satellite imagery) is expensive to acquire. An emerging alternative technique, able to quantify the small-scale (sub-decimeter resolution) topography and landforms of glacier forelands, is through the creation of high resolution orthophotos and DEMs from close range aerial photography obtained from unmanned aerial vehicles (UAVs; Chandler *et al.*, 2015; Evans *et al.*, 2016b; Hackney and Clayton, 2015; Rippin *et al.*, 2015). Once acquired, these photos can be transformed into an elevation model using structure from motion (SfM) techniques (Smith *et al.*, 2016). This enables the rapid collection of high resolution geospatial data at a fraction of the cost of traditional methods.

Here we present an orthophoto and extremely high resolution DEM of the foreland of Isfallsglaciären, Tarfala Valley, Sweden, created from images taken from a UAV. This is used to construct a map of the geomorphology of the foreland. The aims are to: (i) demonstrate how the techniques employed can be successfully used to analyse/record the morphometrics of glacial landforms, in this case flutes; (ii) evaluate the morphological properties of flutes on this foreland, in order to ascertain flute formation mechanisms; and (iii) evaluate the applicability of this approach for studying glacier forelands and glacial geomorphology elsewhere.

Study Site and Previous Work

Isfallsglaciären (67.914°N, 18.572°E) is a small, polythermal glacier situated in the Tarfala valley of the Kebnekaise massif, Swedish Lapland (Figure 1). It takes its name from the ice fall which coincides with the geological boundary between the Kebne dyke complex and Storglaciären gneiss (Andréasson and Gee, 1989). Two parallel moraines mark the limit of the foreland (Figure 1(C)), the innermost of which was overridden by an advance between 1897 and 1916 (Rabot and Muret, 1912, p. 49; Karlén, 1973). Subsequently, the ice margin receded at a rate of ~4 m/a until 1990, since when it has remained at approximately its current position (Orbring, 2002; WGMS FoG database version:2015-11-25). The retreat has revealed a foreland which is currently ~0.6 km^2.

The geomorphology of the foreland has been studied previously by many researchers, which provides a useful comparison with our results, allowing a discussion of the validity of the approach. Hoppe and Schytt (1953) observed flutes on the glacier foreland, and in trenches excavated through the

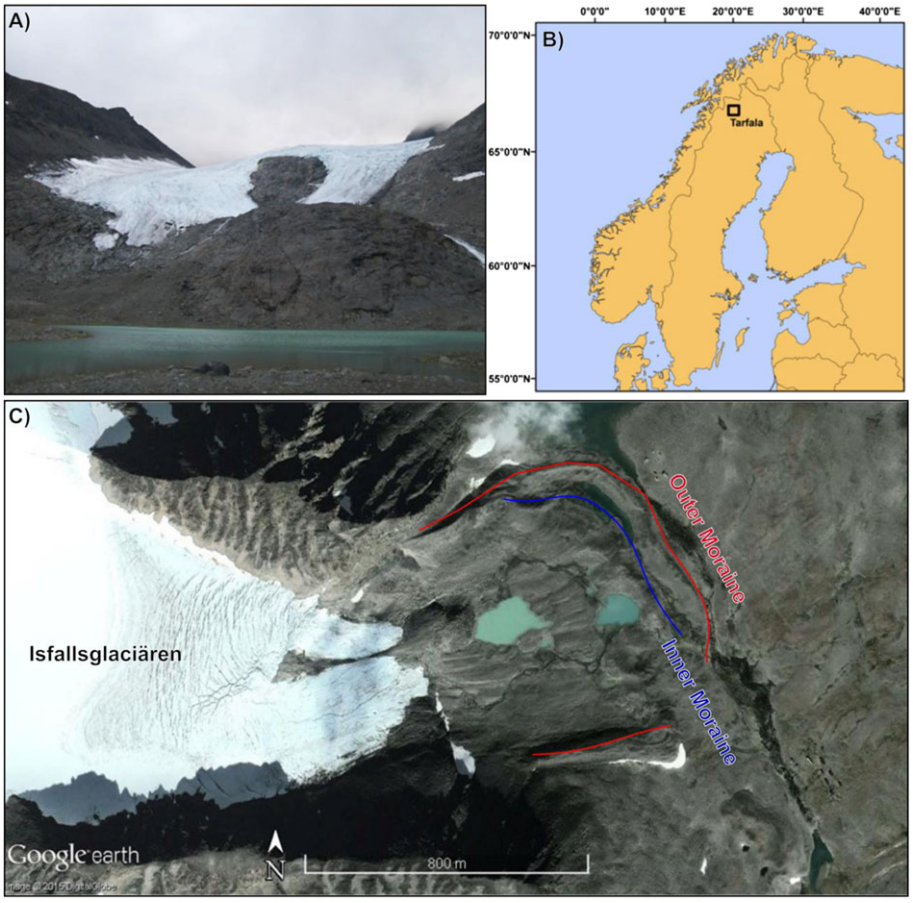

Figure 1. (A) Photo of Isfallsglaciären, taken from the foreland (14/08/2014). The glacier is situated approximately 1300 m above sea level, and is ~500 m wide across its terminus. (B) Location of the Tarfala valley. (C) Satellite image of Isfallsglaciären and its foreland (08/10/2013). This figure is available in colour online at wileyonlinelibrary.com/journal/esp

glacier. They noted 54 regularly spaced flutes on the foreland, 5 to 45 cm in relief. Beneath the glacier, flutes tended to have a greater relief, up to 90 cm high, which Hoppe and Schytt (1953) attributed to the volume of ice they contained. Hoppe and Schytt (1953) proposed that the flutes were formed by the infilling of till into a subglacial cavity generated in the lee-side of a boulder. The cavity infill model was supported by Åmark (1980), who found a correspondence between the initiating boulder geometry and flute geometry. This model, and variants thereof, have also been proposed for other flute fields (Dyson, 1952; Paul and Evans, 1974; Boulton, 1976; Morris and Morland, 1976; Benn, 1994; Roberson *et al*., 2011), although alternative formation hypotheses exist (Baranowski, 1970; Gordon *et al*., 1992; Schoof and Clarke, 2008). Eklund and Hart (1996) studied the sedimentology of a single flute on the Isfallsglaciären foreland, concluding that this flute was formed by the infilling of sediment into the lee-side of a boulder, but highlighted the role of subglacial sediment deformation in this process. In a synthesis of the retreat of glaciers in the Kebnekaise massif, Karlén (1973) also mapped the foreland of Isfallsglaciären from aerial photography, but did not map its flutes. Karlén (1973) mapped a small esker on the foreland, and marked the position of several dry proglacial channels, as well as outwash sediments being deposited in proglacial lakes. Carrivick *et al*. (2015) used a terrestrial laser scanner to produce a freely available 1 m grid cell resolution DEM of the upper portion of the Tarfala valley, including the foreland of Isfallsglaciären. This dataset, and the previous accounts of the foreland geomorphology, provides us with comparisons to validate our method.

Methods

Data acquisition

Our survey was conducted on 14/08/2014. Images of Isfallsglaciären foreland were taken using a Nikon D5300 24 megapixel digital single-lens reflex camera, attached to a servo controlled gimbal mounted on a custom built DroidWorx Hexacopter (Figure 2). The camera lens was fixed at 18 mm focal length to allow for a constant field of view and to maximise image overlap. The shutter was radio controlled, taking images approximately every 3 seconds. Each image was geotagged using a GPS mounted to the UAV. The UAV was flown at altitudes of 100–120 m and utilised automatic stabilisation and controlled descent. This enabled the hexacopter to remain stable in wind speeds of 15 km/h.

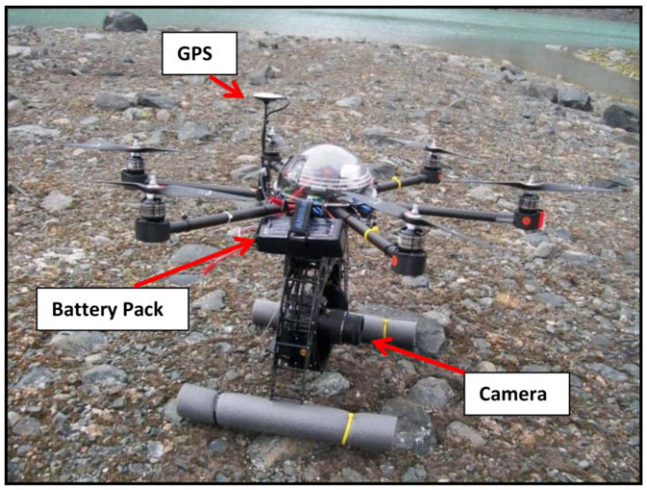

Figure 2. The hexacopter with key components labelled. This figure is available in colour online at wileyonlinelibrary.com/journal/esp

In total, 23 ground control points (GCPs) were surveyed with a dGPS (Lecia System 1200 GPS). GCPs included prominent boulders which had previously been marked with paint, or white targets placed on the ground. Photos of each GCP were taken in the field to later help identification. Points were surveyed using a GPS rover, and were relayed a short distance (~1 km) to a GPS base station located over a known point (Research Station, ETRS89 BM). The GPS data were then processed in Leica GeoOffice software giving GCP position accuracies below 0.05 m.

Data processing

Our data processing procedure is similar to that of Evans *et al*. (2016b), and is summarised in Figure 3. Image processing was conducted in AgiSoft PhotoScan Professional, one of the most widely used SfM software packages (Chandler *et al*., 2015; Evans *et al*., 2016b; Ryan *et al*., 2015). All images were judged to be clear and sharp enough to warrant processing ($n = 836$). The photos were divided between two groups (termed 'chunks' in Agisoft), which roughly split the study area geographically in half. These were processed separately and then merged to increase processing speed (Figure 3). Images were initially aligned through the geotagged GPS positions and automatically detected common points between overlapping images (Figure 3). GCPs were then identified on the aligned images and used to re-align the images and chunks. A dense network of elevation point measurements was then calculated. Errors created at abrupt surface property changes (e.g., at proglacial lakes), and over field equipment or people, were masked out of DEM processing. A point cloud containing >23.3 million points spaced approximately 0.1 m apart was created (Figure 3). From this, a triangular irregular network (TIN) mesh was built, and was used as the basis of our DEM and for orthorectification of the aerial photography.

The resultant orthophoto has a horizontal pixel resolution of 2 cm (Figure 4(A)). The DEM (Figure 4(B)) has the same resolution, interpolated using inverse distance weighting from our TIN. The orthophoto has a root mean square locational error of ~4 cm relative to the GCPs and the root mean square error of the DEM compared the GCPs is ~5 cm, comparable with the accuracy of the dGPS measurements. Although these positional and relative vertical accuracies are high, both decrease slightly away from the GCPs. Furthermore, regions of increased error exist due to high reflection off shallow water features, where the processing was split into two regions, and where image quality was reduced. However, the overall result is an unprecedentedly detailed DEM of the glacier foreland (Figure 4). Both products are projected using the Swedish Reference Frame 1999 Transverse Mercator projection and the RH2000 Geoid (SWEREF_2000).

Mapping and metrics

A geomorphological map of the foreland of Isfallsglaciären was created in ArcGIS v.10.1 using the exported orthophoto and DEM. The orthophoto was locally contrast-stretched; a technique which has proven useful for highlighting subtle features on satellite imagery (Ely and Clark, 2016). The DEM was hillshaded from multiple angles (315°, 45° and above) to avoid azimuth biasing, a visualisation technique regularly used for the mapping of subglacial bedforms (Smith and Clark, 2005; Hillier *et al*., 2015).

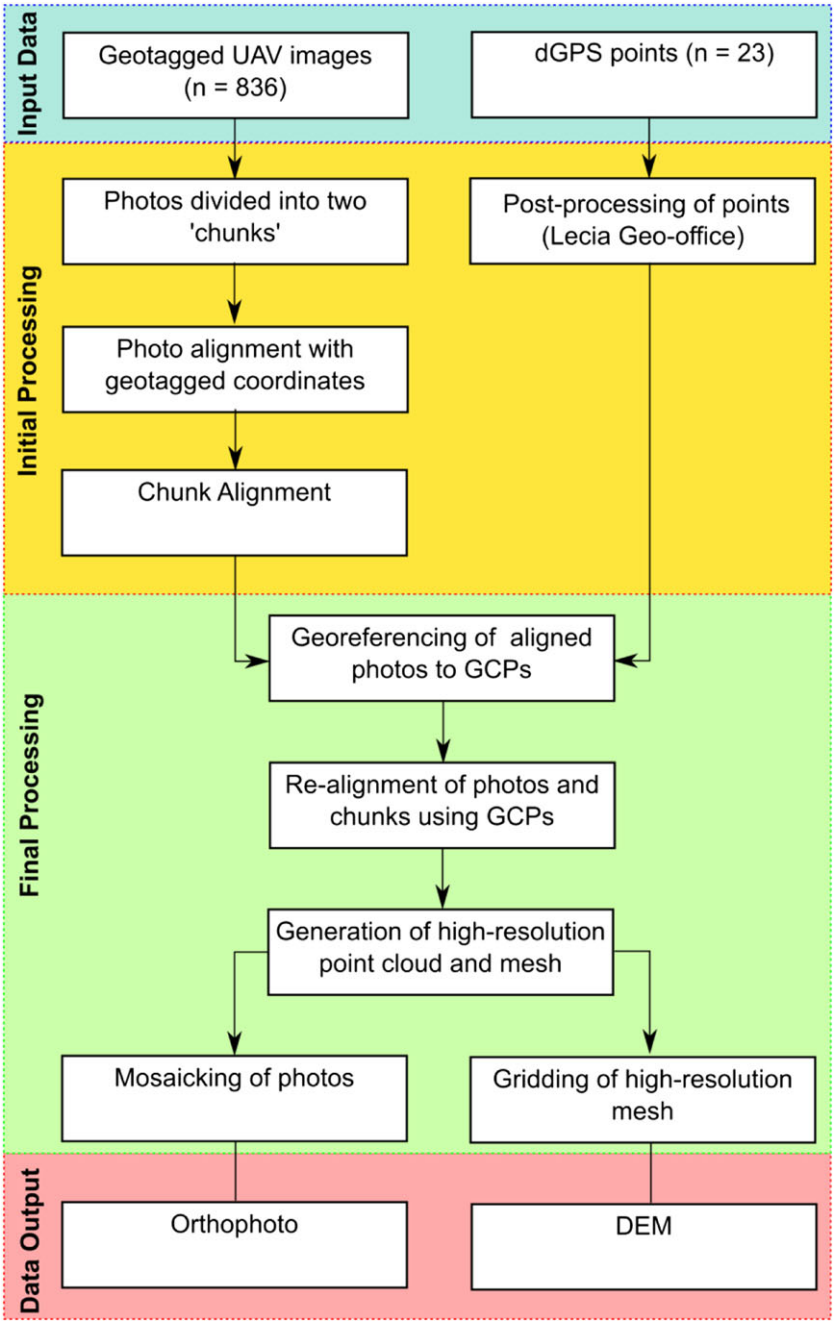

Figure 3. Overview of data processing workflow. This figure is available in colour online at wileyonlinelibrary.com/journal/esp

Flutes were mapped from the DEM along their crest line, defining flute length. Any boulder at the stoss-end of the flute was mapped as a point, defining its highest elevation. Flute width and relief were measured by taking the average of cross-profile values at three points along the flute crest; roughly at 10, 50 and 90% of the flute-length. Where the flutes sit on a sloped surface, the cross-profiles were detrended in order to measure flute relief (Spagnolo *et al.*, 2012). Large boulders on top of the flutes were avoided when placing cross-profiles. The relief and across-flow width of each initiating boulder was also measured using cross-profiles.

Results

The geomorphological map produced from our orthophoto and DEM (Figure 5) highlights a range of geomorphological features across the foreland. The largest geomorphological feature captured is the inner moraine mentioned in the second section (Figure 5). The outermost moraine (Figure 1), which marks the limit of the foreland, was not surveyed. The inner moraine is ~16 m in relief decreasing to the NNW to ~8 m (Figure 5). The inner moraine is fluted to the NNW, coinciding with the region where its relief is reduced. Inside the inner moraine, closer to the glacier front, the foreland is fluted (Figures 5 and 6(A)). These flutes are superimposed on larger mounds of sediment, approximately 1 to 3 m in relief and a few tens of meters wide (Figures 5 and 6(B)). Whether these mounds were formed sub- or pro-glacially is unclear, but the dry v-shaped channels between the ridges suggest that water has acted to excavate the inter-ridge areas. These channels were also noted by Karlén (1973), and the arrangement of these mounds was noted in Carrivick *et al.* (2015).

Examples of detail visible in the orthophoto and DEM are shown in Figure 7. The high resolution of the imagery and DEM means even flutes as small as 16 cm wide are discernible (e.g. Figure 7(A) and (B)). Channels cut into the foreland are also visible on the DEM (e.g. Figures 7(C), 7(D) and 5). These

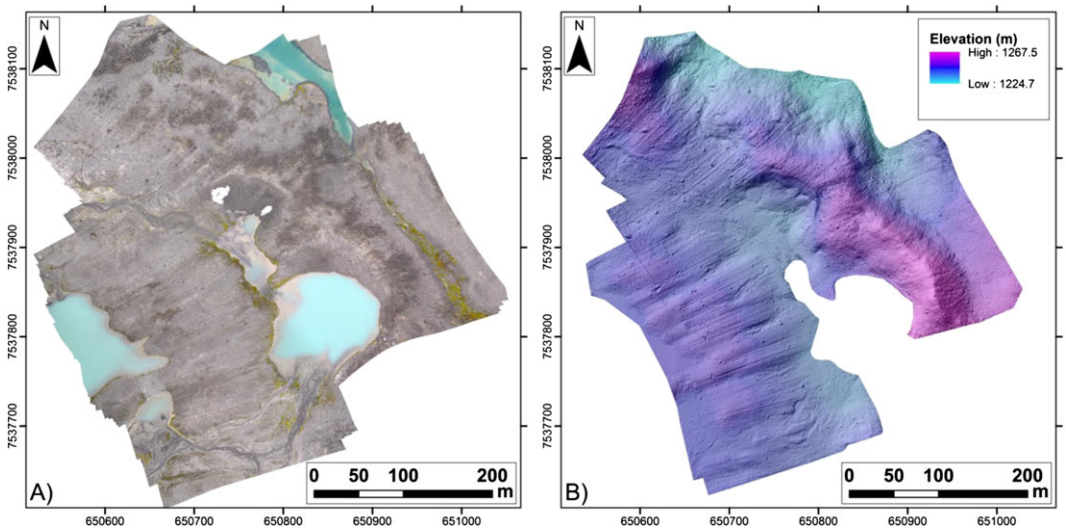

Figure 4. (A) Orthophoto of the foreland. (B) DEM of the foreland, with a transparent hill-shade from the north-west applied. Co-ordinates in SWEREF99_TM. This figure is available in colour online at wileyonlinelibrary.com/journal/esp

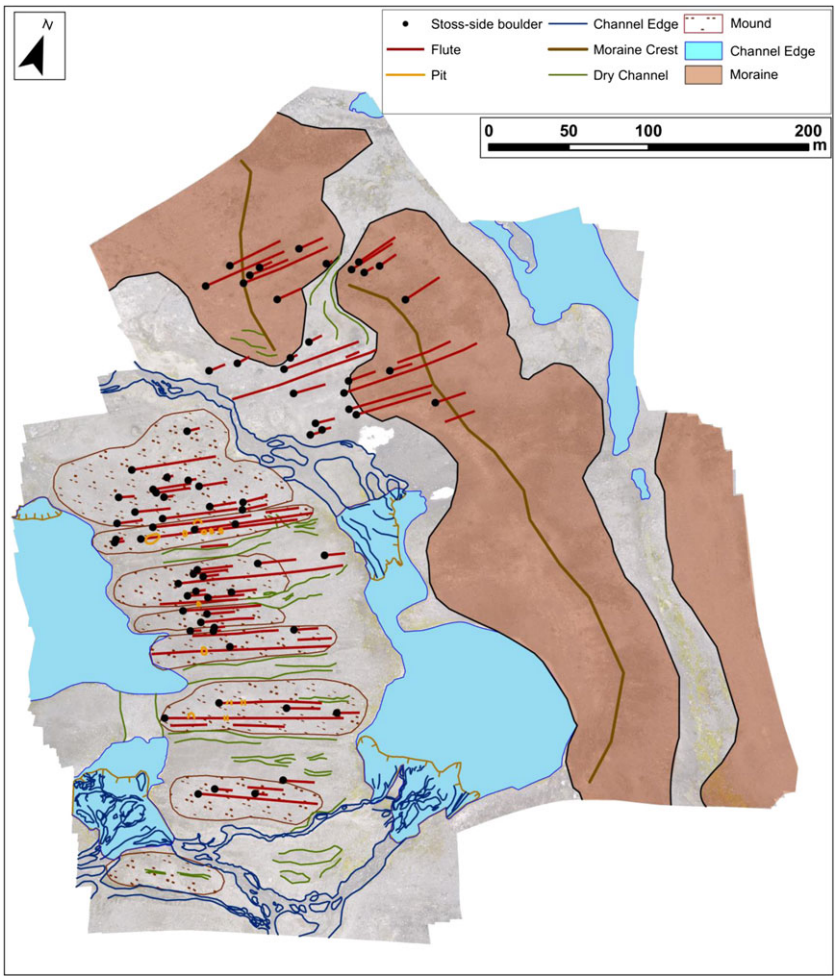

Figure 5. Geomorphological map of the foreland of Isfallsglaciären. Background is a transparent image of the orthophoto. Note that the map has been rotated 20° anti-clockwise. This figure is available in colour online at wileyonlinelibrary.com/journal/esp

channels connect the proglacial lakes, transferring sediment and forming fans as they flow in (Figures 4(A) and 5). Information on the submerged fans is limited to the orthophoto (Figure 4(A)), as elevation data of the lake bed could not be created over the water bodies. Human impacts on the foreland can also be seen in the data, with several pits excavated by previous expeditions, visible in both the orthophoto and DEM (Figures 7(E), 7(F) and 5).

In total, 88 flutes were mapped across the study area. On average, the measured flutes are approximately 28 m long (Table I; Figure 8(A)). However, flute length is variable exhibiting a large range (Table I). This is reflected in the probability distribution function (PDF), which is positively skewed (Figure 8(A)). Flute width is more constrained, with distinct neighbouring modal classes of 125–175 cm (Figure 8(B)) and a probability distribution function closer to a normal

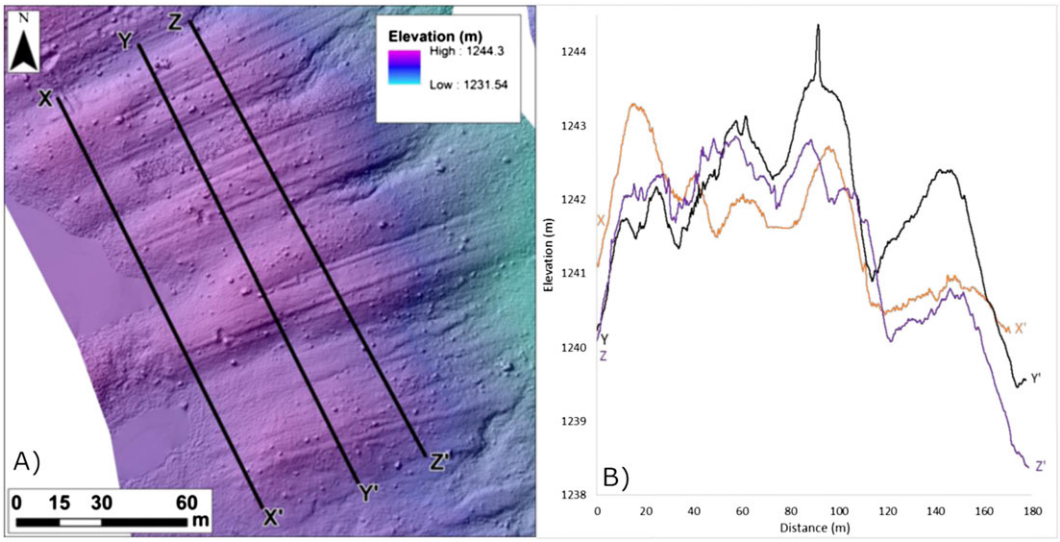

Figure 6. (A) The inner flute field. Note how the flutes sit on top of larger sediment mounds. (B) Transects across the flute field, located on (A). Note how the individual flutes appear as spikes over the longer wavelength (~ 50 m wide) topography. This figure is available in colour online at wileyonlinelibrary.com/journal/esp

distribution. Impressively, flutes only 2 cm in relief were measured, demonstrating the vertical resolution of the data (Table I). Flute relief was most commonly found to be 2–4 cm, with a tail to the distribution after this modal class (Figure 8 (C)). Elongation ratio (length/width) retains the positive skew of the length measurement (Figure 8(D)), with flutes reaching nearly 100 times as long as they are wide (Table I).

Initiating boulders were mapped for 85% of the flutes (Figure 5). For the remaining flutes, we cannot rule out a buried initiating boulder (IB), or erosion leading to disassociation between an IB and the flute. Flute width has a strong positive correlation with the width of an IB (Figure 9(A)). Flutes with larger relief have higher IBs (Figure 9(B)). The wider the flute, the greater its relief (Figure 9(C)). However, relationships between boulder height and flute length (Figure 9D) and flute length and width (Figure 9(E+) are much weaker.

The technique also compares favourably with other methods of geospatial data capture. The DEM produced is of a higher resolution than that created by Carrivick *et al.* (2015) through terrestrial laser scanning (note that the aim of Carrivick *et al.* (2015) was to survey the entire Tarfala valley, rather than just one foreland). Although both techniques have their merits and limitations, importantly the greater resolution of our DEM allowed us to accurately record the dimensions of the flutes in a way that is not possible with the DEM of Carrivick *et al.* (2015) (Figure 10). We found only 20 clear examples of flutes across the study area from the terrestrial lidar scanning DEM, and these correspond to the longest flutes of our analysis (Figure 10(C)). The coarser resolution lidar DEM also leads to an overestimation of flute width (Figure 10(D)). Furthermore, the precise identification of initiating boulders is made easier with the UAV-based DEM, especially when these are of modest size (Figure 10(A) and (B)).

Discussion

Comparison with other studies and utility of approach

The techniques employed here enabled rapid capture of aerial photos and the production of a high resolution orthophoto and DEM of the foreland of Isfallsglaciären. The main advantage of this technique is that it has allowed us to define the morphology of more small landforms (flutes) than previous field-based studies. Our data captured the morphometrics of 88 flutes, compared with the 21 reported by Åmark (1980).The narrowest flute (16 cm) recorded here compares well with the narrowest found by the field based study of Åmark (1980) (20 cm), suggesting that our horizontal resolution is sufficient for defining flute morphology. At Turtmann Glacier, Switzerland, van der Meer (1997) reported much smaller 'mini-flutes,' which were less than 20 cm wide and 10 cm high. The orthophoto resolution is sufficient to resolve features of this scale so they are assumed absent from the study area. However, the cut off in relief measurements below 2 cm (Figure 8(C)) may be a consequence of DEM resolution. Therefore, if extremely small-scale geomorphological features are present, field measurement or further DEM refinement would be required but should still be mappable on the orthophoto.

Flute metrics and formation mechanisms

As demonstrated above (Figures 8 and 9), a major advantage of our technique is the ability to image and obtain the morphometrics of even small (~2 cm relief) flutes and any initiating boulder. Morphological studies of other subglacial bedforms, involving the study of thousands of features, have provided useful insights into their formation and provide constrains for numerical models (Dunlop and Clark, 2006; Clark *et al.*, 2009; Spagnolo *et al.*, 2014; Ely *et al.*, 2016). However, the need for high resolution DEMs, of the type demonstrated here, has meant that flutes have evaded such a study.

The data presented here shows that the majority of flutes at Isfallsglaciären have an initiating stoss-side boulder (85%). The width of an IB has a strong positive relationship with width of the flute formed in its lee (Figure 9(A)). The height of an IB also displays a positive relationship with flute height (i.e. higher, wider IBs have higher, wider flutes) (Figure 9(B)). This is consistent with the lee-side cavity infill mechanism of flute formation that has been proposed for flutes at Isfallsglaciären and elsewhere (Dyson, 1952; Paul and Evans, 1974; Boulton, 1976; Morris and Morland, 1976; Benn, 1994; Roberson *et al.*, 2011). A cavity forms at the sole of the glacier which infills with sediment as the ice slides over the IB, forming the

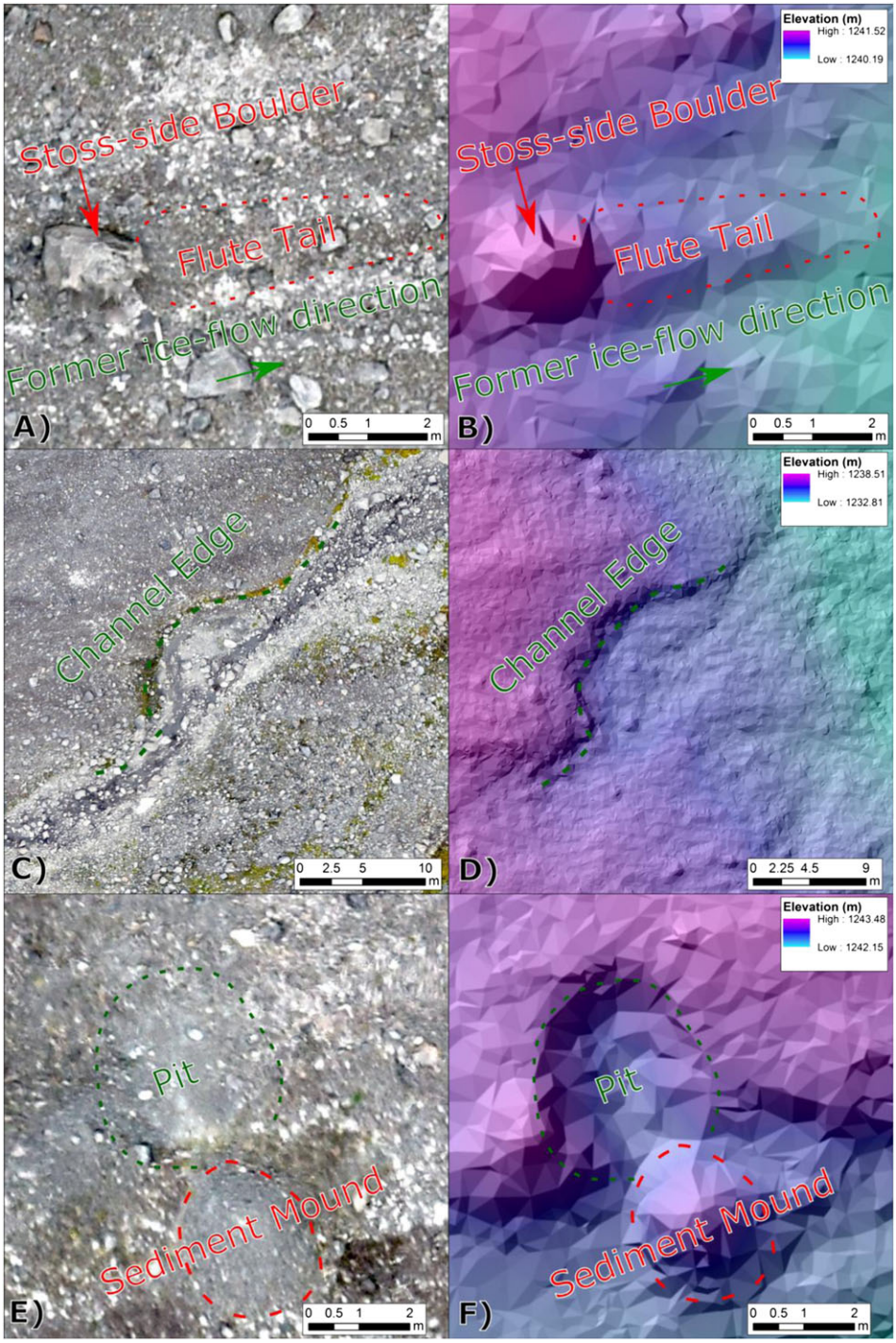

Figure 7. Smaller scale features discernible on the foreland. Orthophoto is on the left and hill-shaded DEM is on the right. (A) and (B) A short flute and its initiating boulder. (C) and (D) A proglacial channel. (E) and (F) An exposed pit and the pile of excavated sediment. This figure is available in colour online at wileyonlinelibrary.com/journal/esp

Table I. Flute size and shape metrics.

	Minimum	Maximum	Mean	Standard Deviation
Length (m)	4.0	112.0	28.0	±25.9
Width (cm)	16	368	147	±68
Elongation ratio (Length/Width)	2.9	98	20	±16
Relief (cm)	2	30	10	±7

flute. This cavity is likely maintained by the freezing of sediment behind the initiating boulder (Roberson *et al.*, 2011).

Of the 88 flutes identified, 15% had no observable IB. For these, it is plausible that an IB has been hidden due to burial by sediment or submergence in the proglacial lakes (e.g. Figure 11(A)). Alternatively, boulders may have been removed/displaced during glacial retreat or following deglaciation, meaning that they are no longer aligned with the flutes they formed (e.g. Figure 11(B)). For the flutes at Isfallsglaciären, we therefore find no need to invoke hypotheses which require no initiating boulder. However, a much larger dataset, spanning a variety of glacier forelands, should be analysed before a definitive and generalised conclusion on flute formation is drawn. The hypotheses that do not require initiating boulders include frost heave, rather than boulders, generating subglacial obstructions (with associated lee-side cavities) (Baranowski, 1970) or mechanisms which involve basal ice flow instabilities (Schoof and Clarke, 2008).

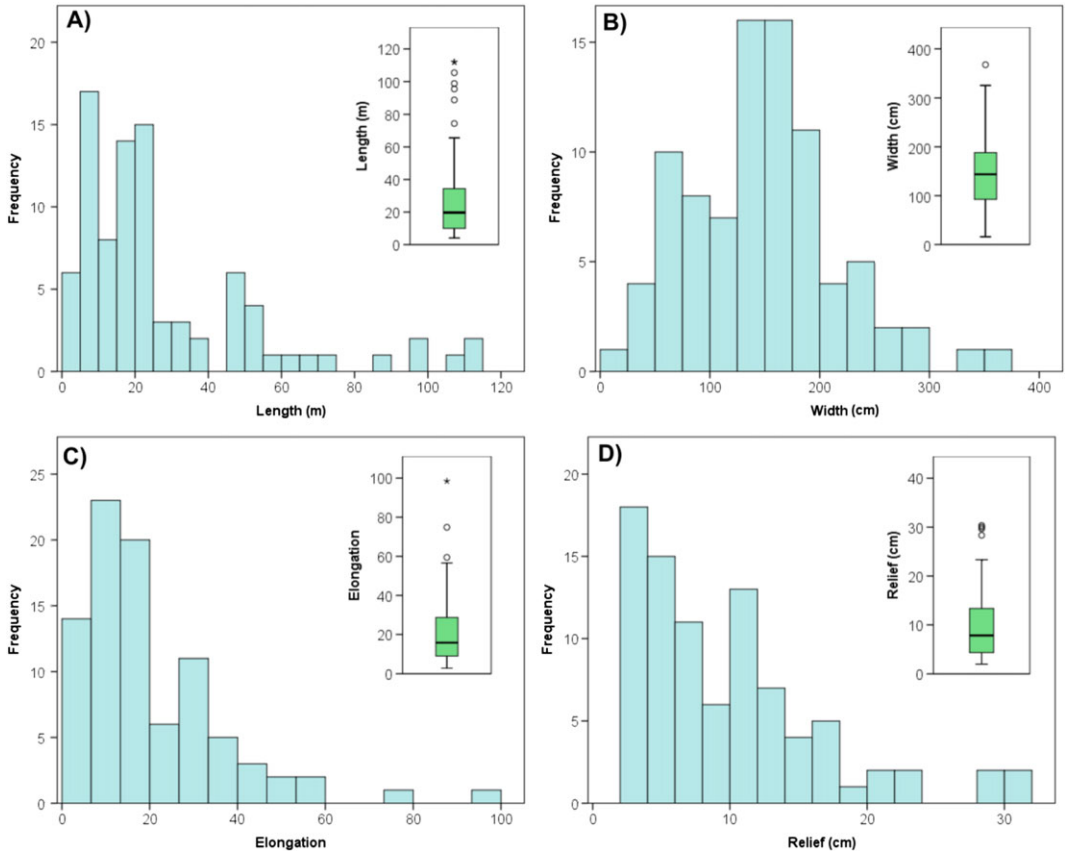

Figure 8. Histograms and box and whisker plots of flute size and shape metrics. This figure is available in colour online at wileyonlinelibrary.com/journal/esp

While boulder geometry has a relationship with flute width and height (Figure 9(A) and (B)), there is little correspondence between the boulder height and flute length (Figure 9(D)) or between flute width and flute length (Figure 9(E)). No spatial trends in flute length were observed that would suggest that parameters such as ice thickness or velocity (Hart, 1999) control the flute length. One possibility is that erosion across the foreland has masked any spatial trends in flute length. Alternatively, sediment supply could have influenced flute length, and therefore shorter flutes were more rapidly starved of sediment. The lack of relation between boulder height and flute length (Figure 9(D)), and flute width and length (Figure 9(E) shows that larger cavities (larger boulders with wider flutes), did not grow longer by attracting and freezing more sediment at the expense of smaller cavities (smaller boulders with narrower flutes). These larger cavities would also require more sediment to fill and freeze into the cavity, in order for it to propagate and lengthen a flute.

An alternative explanation for the mixed length of flutes could be that they are of a mixed age. If the IBs became lodged at different times, each flute is independent of the others, and shorter flutes simply had less time to develop. An analogue for this may be found at the Dubwant Lake ice stream, where shorter lineations were interpreted to be younger than neighbouring longer lineations (Stokes *et al.*, 2013). Likewise, Evans and Rea (2003) interpreted short flutes to be late stage features produced at the termination of a surge of Brúarjöklull, Iceland. Similar arrangements (short flutes neighbouring long flutes) have also been found for flutes elsewhere (Kjær *et al.*, 2006). Growth of subglacial bedforms has been invoked to explain the exponential or long normal distribution of their size metrics (Fowler *et al.*, 2013; Hillier *et al.*, 2013). The PDF of flute lengths at Isfallsglaciären is positively skewed (Figure 8 (A)), but the low sample size makes it difficult to attribute either an exponential or log-normal shape to this distribution. A larger sample of flutes, from a bigger geographical area or multiple fluting fields would help resolve this.

Beneath the glacier, Hoppe and Schytt (1953) recorded flutes that were 90 cm in relief, with a high ice content. These flutes are now exposed, and our data records a maximum flute height of 30 cm (Table I). This height reduction is likely a consequence of the ice melt or dewatering from within the flute sediment after exposure, which led to till compaction. Flutes in the foreland were found to be typically 25% of the height of the stoss-side boulder. If it is assumed, as the cavity infill model suggests, that the original height of the flutes were close to that of the initiating boulders, then we can argue that up to 75% of their original flute volume is composed of water or ice.

Overall, for the flutes at Isfallsglaciären we agree with previous studies (Hoppe and Schytt, 1953; Åmark, 1980; Eklund and Hart, 1996) and favour formation via the infill of a propagating cavity in the lee of an IB. Flute formation in a propagating cavity behind a boulder could explain why flutes are much narrower than all other subglacial bedforms, sitting outside a subglacial bedform continuum (Ely *et al.*, 2016). Perhaps this scale specificity is due to the size of boulders available for flute genesis in forelands in combination with sediment availability. However, whether the lee-side cavity infill mechanism can be extended to all flutes (i.e. monogenesis), or whether several formation mechanisms are required (i.e. polygenesis) is unknown. If applied elsewhere, the geospatial data capture technique has the potential to address this issue, by tacking the following questions: (i) Do flute metrics vary between forelands? (ii) How prevalent are flutes without initiating boulders? (iii) Does the initiating boulder always control flute morphology? (iv) Does flute morphology indicate that they grow by propagating down flow (Fowler *et al.*, 2013; Hillier *et al.*, 2013)?

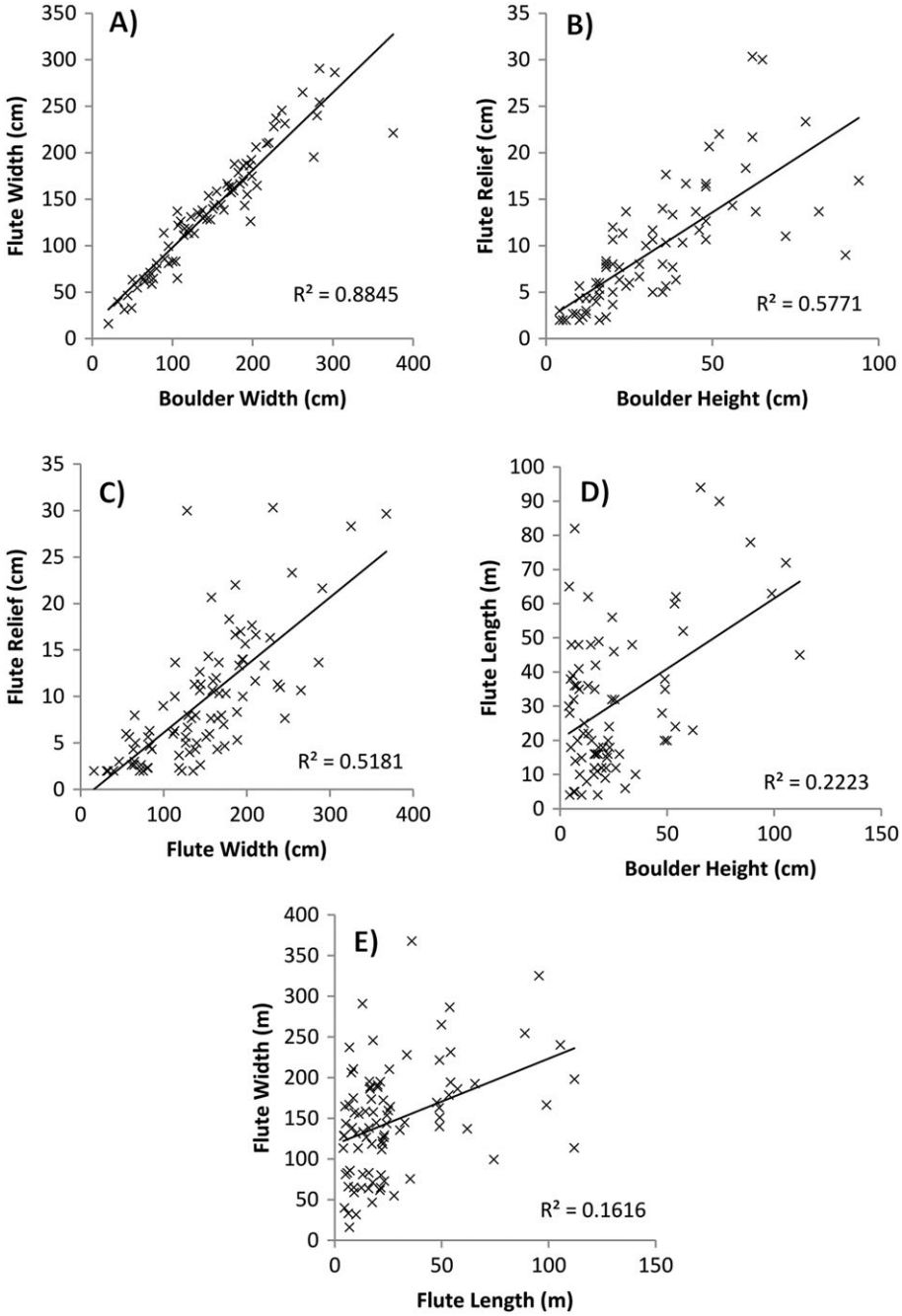

Figure 9. Relationships between measured flute and boulder metrics. This figure is available in colour online at wileyonlinelibrary.com/journal/esp

Recommendations and future directions

As shown here, and in previous studies (Chandler *et al.*, 2015; Evans *et al.*, 2016b), UAVs provide a robust method for capturing geospatial data over glacier forelands. However, there are some disadvantages to using UAVs in glacial environments which should be taken into consideration for future work. For example, spatial coverage was necessarily limited, due to weather conditions. The UAV used could not fly in high winds, and rain not only infiltrates the electrics, but can cause a haze in photography. Poor visibility due to low cloud was also an issue. Therefore, for many mountainous glacial environments, UAV based data capture may be challenging and require extra acquisition time, especially in poor weather conditions. That said, the quick set-up and take off time of the UAV is well suited to the small time-windows of suitable weather that are common in such environments and new UAVs are improving their reliability even under adverse weather conditions. As the computing time required to process the data is relatively high, computing should be avoided while in the field and multi-processor or cluster computers are recommended. It is worth noting that user input is limited to choosing options between processing stages, and that software is becoming increasingly user friendly (Smith *et al.*, 2016).

Despite these shortcomings, UAV based SfM photography capture provides a rapid option for generating incredibly high resolution data of glacier forelands. A clear avenue for future research would be to use UAVs to monitor foreland change through repeat surveying of the foreland (Evans *et al.*, 2016a; Chandler *et al.*, 2016). Given that flutes (Rose, 1991), and other landforms found on glacier forelands, are likely to be rapidly modified after exposure, repeat measurements of recently deglaciated forelands may provide quantification of landform modification after exposure. Furthermore, the rapidity of the technique allows for multiple sites to be monitored in a single field season, allowing large areas to be mapped in detail.

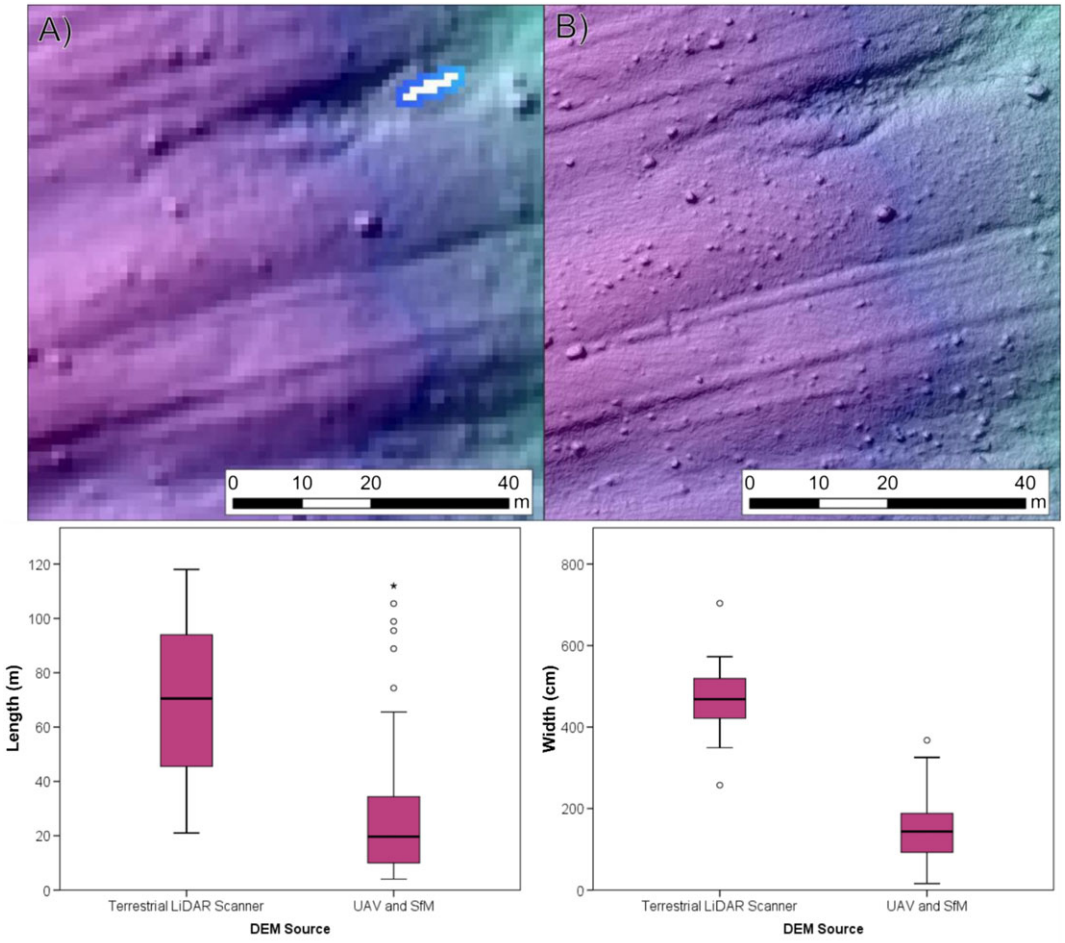

Figure 10. Comparison between (A), the ~1 m DEM of Carrivick *et al.* (2015), and (B) the ~2 cm DEM presented here. While flutes are visible in (A), they appear sharply in (B) enabling their size and shape metrics to be more precisely determined. Both images are hill-shaded from the north-west. Comparative box plots of flute length (C) and width (D) derived from two different DEMs. This figure is available in colour online at wileyonlinelibrary.com/journal/esp

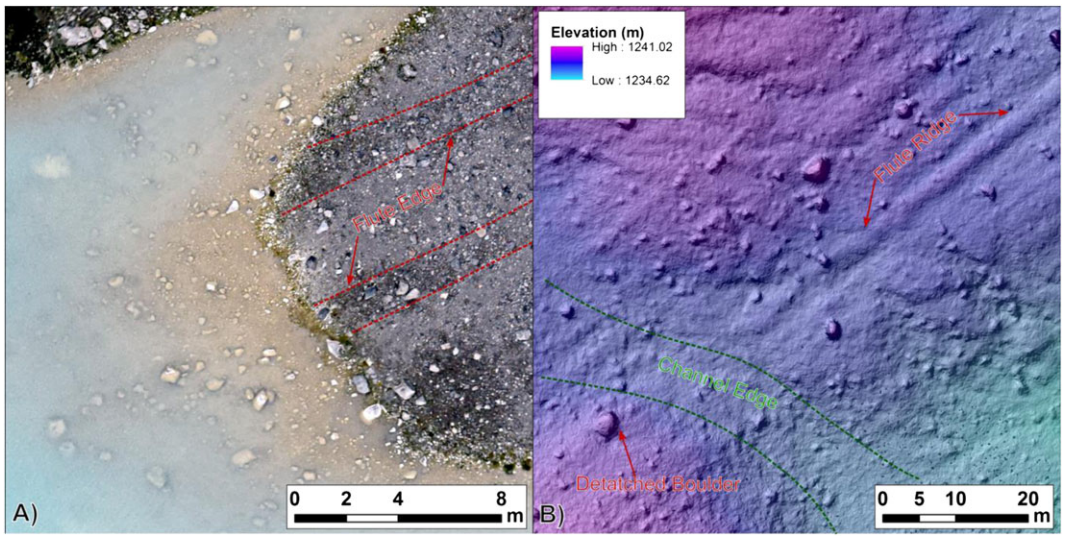

Figure 11. Examples of boulder-less flutes. (A) Orthophoto of flutes emerging from a proglacial lake. (B) Hill-shaded DEM of a flute which may have become detached from its initiating boulder, due to a proglacial stream. This figure is available in colour online at wileyonlinelibrary.com/journal/esp

Conclusions

Here we document the creation of an orthophoto and DEM of the foreland of Isfallsglaciären. The data produced are of an extremely high horizontal resolution (2 cm), and relative vertical accuracy (~ 5 cm). This enabled mapping of the glacier foreland, and the subglacial flutes in particular, in unpreceded detail. The use of SfM methods on photography acquired from UAVs is therefore a useful approach for geomorphological mapping of various landforms, including extremely small ones. Importantly, the DEM enables the recording of the morphological properties of flutes not discernible from other sources. Most

mapped flutes are characterised by the presence of an initiating boulder, with flute morphology directly related to boulder size. This is consistent with the cavity infill model of flute formation. If applied elsewhere, we suggest that the technique could provide useful insights into the origin of flutes and potentially other landforms found on glacier forelands.

Acknowledgments—The research leading to these results has received funding from the European Union Seventh Framework Programme (FP7/2007-2013) under grant agreement no. 262693 (INTERACT). This work was also supported by an equipment loan from the NERC Geophysical Equipment Facility (loan number 1008). The authors would like to thank the Tarfala research station staff. J.C.E would like to thank the Denisons for supporting his PhD. We would also like to thank Jonathan Carrivick, Mark Smith and Daniel Carrivick for access to their DEM. Chris Clark is thanked for his support of the project and for useful discussions. The authors also thank the two reviewers and the editorial team for their comments which improved this manuscript.

References

Åmark M. 1980. Glacial flutes at Isfallsglaciären, Tarfala, Swedish Lapland. *Journal of the Geological Society of Sweden* **102**(3): 251–259.

Andréasson PG, Gee DG. 1989. Bedrock geology and morphology of the Tarfala area, Kebnekaise Mts., Swedish Caledonides. *Geografiska Annaler. Series A Physical Geography* 235–239.

Baranowski S. 1970. The origin of fluted moraine at the fronts of contemporary glaciers. *Geografiska Annaler. Series A. Physical Geography* **52**(1): 68–75.

Barr ID, Clark CD. 2009. Distribution and pattern of moraines in Far NE Russia reveal former glacial extent. *Journal of Maps* **5**(1): 186–193.

Benn DI. 1994. Fluted moraine formation and till genesis below a temperate valley glacier: Slettmarkbreen, Jotunheimen, southern Norway. *Sedimentology* **41**(2): 279–292.

Bennett MR, Hambrey MJ, Huddart D, Ghienne JF. 1996. The formation of a geometrical ridge network by the surge-type glacier Kongsvegen, Svalbard. *Journal of Quaternary Science* **11**(6): 437–449.

Boulton GS. 1976. The origin of glacially fluted surfaces Á/observations and theory. *Journal of Glaciology* **17**(76).

Bradwell T, Stoker MS, Golledge NR, Wilson CK, Merritt JW, Long D, Everest JD, Hestvik OB, Stevenson AG, Hubbard AL, Finlayson AG. 2008. The northern sector of the last British Ice Sheet: maximum extent and demise. *Earth-Science Reviews* **88**(3): 207–226.

Carrivick JL, Smith MW, Carrivick DM. 2015. Terrestrial laser scanning to deliver high-resolution topography of the upper Tarfala valley, arctic Sweden. *Journal of the Geological Society of Sweden* **137**(4): 383–396.

Chandler BM, Evans DJ, Roberts DH, Ewertowski M, Clayton AI. 2015. Glacial geomorphology of the Skálafellsjökull foreland, Iceland: a case study of 'annual'moraines. *Journal of Maps*: 1–13.

Chandler BM, Evans DJ, Roberts DH. 2016. Characteristics of recessional moraines at a temperate glacier in SE Iceland: insights into patterns, rates and drivers of glacier retreat. *Quaternary Science Reviews* **135**: 171–205.

Clark CD. 1993. Mega-scale glacial lineations and cross-cutting ice-flow landforms. *Earth Surface Processes and Landforms* **18**(1): 1–29.

Clark CD, Hughes AL, Greenwood SL, Spagnolo M, Ng FS. 2009. Size and shape characteristics of drumlins, derived from a large sample, and associated scaling laws. *Quaternary Science Reviews* **28**(7): 677–692.

Dunlop P, Clark CD. 2006. The morphological characteristics of ribbed moraine. *Quaternary Science Reviews* **25**(13): 1668–1691.

Dyson JL. 1952. Ice-ridged moraines and their relation to glaciers [Montana]. *American Journal of Science* **250**(3): 204–211.

Eklund A, Hart JK. 1996. Glaciotectonic deformation within a flute from the Isfallsglaciären, Sweden. *Journal of Quaternary Science* **11**(4): 299–310.

Ely JC, Clark CD. 2016. Flow-stripes and foliations of the Antarctic ice sheet. *Journal of Maps* **12**(2): 249–259.

Ely JC, Clark CD, Spagnolo M, Stokes CR, Greenwood SL, Hughes ALC, Dunlop P, Hess D. 2016. Do subglacial bedforms comprise a size and shape continuum? *Geomorphology* **257**: 108–119.

Etzelmüller B, Ødegård RS, Vatne G, Mysterud RS, Tonning T, Sollid JL. 2000. Glacier characteristics and sediment transfer system of Longyearbreen and Larsbreen, western Spitsbergen. *Norsk Geografisk Tidsskrift* **54**(4): 157–168.

Evans DJA, Rea BR. 1999. Geomorphology and sedimentology of surging glaciers: a land-systems approach. *Annals of Glaciology* **28**(1): 75–82.

Evans DJA, Rea BR. 2003. Surging glacier landsystems. In *Glacial Landsystems*, Evans DJA (ed). Arnold: London; 259–284.

Evans DJ, Twigg DR, Rea BR, Shand M. 2007. Surficial geology and geomorphology of the Brúarjökull surging glacier landsystem. *Journal of Maps* **3**(1): 349–367.

Evans DJA, Nelson CD, Webb C. 2010. An assessment of fluting and 'till esker' formation on the foreland of Sandfellsjökull, Iceland. *Geomorphology* **114**(3): 453–465.

Evans DJA, Ewertowski M, Jamieson SS, Orton C. 2016a. Surficial geology and geomorphology of the Kumtor Gold Mine, Kyrgyzstan: human impacts on mountain glacier landsystems. *Journal of Maps* **12**(5): 757–769.

Evans DJA, Ewertowski M, Orton C. 2016b. Fláajökull (north lobe), Iceland: active temperate piedmont lobe glacial landsystem. *Journal of Maps* **12**(5): 777–789.

Fowler AC, Spagnolo M, Clark CD, Stokes CR, Hughes ALC, Dunlop P. 2013. On the size and shape of drumlins. *GEM - International Journal on Geomathematics* **4**(2): 155–165.

Gordon JE, Whalley WB, Gellatly AF, Vere DM. 1992. The formation of glacial flutes: assessment of models with evidence from Lyngsdalen, North Norway. *Quaternary Science Reviews* **11**(7): 709–731.

Hackney C, Clayton AI. 2015. Section 2.1.7: Unmanned aerial vehicles (UAVs) and their application in geomorphic mapping, In *Geomorphological Techniques* (Online Edition), Clarke L (ed.). British Society for Geomorphology: London. ISSN: 2047–0371.

Hart JK. 1995. Subglacial erosion, deposition and deformation associated with deformable beds. *Progress in Physical Geography* **19**(2): 173–191.

Hart JK. 1999. Identifying fast ice flow from landform assemblages in the geological record: a discussion. *Annals of Glaciology* **28**(1): 59–66.

Hillier JK, Smith MJ, Clark CD, Stokes CR, Spagnolo M. 2013. Subglacial bedforms reveal an exponential size–frequency distribution. *Geomorphology* **190**: 82–91.

Hillier JK, Smith MJ, Armugam R, Barr I, Boston CM, Clark CD, Ely J, Fankl A, Greenwood SL, Gosselin L, Hättestrand C, Hogan K, Hughes ALC, Livingstone SJ, Lovell H, McHenry M, Muñoz Y, Pellicer XM, Pellitero R, Robb C, Roberson S, Ruther D, Spagnolo M, Standell M, Stokes CR, Storrar R, Tate NJ, Wooldridge K. 2015. Manual mapping of drumlins in synthetic landscapes to assess operator effectiveness. *Journal of Maps* **11**(5): 719–729.

Hoppe G, Schytt V. 1953. Some observations on fluted moraine surfaces. *Geografiska Annaler* **35**(2): 105–115.

Irvine-Fynn TDL, Barrand NE, Porter PR, Hodson AJ, Murray T. 2011. Recent high-arctic glacial sediment redistribution: a process perspective using airborne lidar. *Geomorphology* **125**(1): 27–39.

Iverson NR, Semmens DJ. 1995. Intrusion of ice into porous media by regelation: a mechanism of sediment entrainment by glaciers. *Journal of Geophysical Research: Solid Earth (1978–2012)* **100**(B6): 10219–10230.

Jónsson SA, Schomacker A, Benediktsson ÍÖ, Ingólfsson Ó, Johnson MD. 2014. The drumlin field and the geomorphology of the Múlajökull surge-type glacier, central Iceland. *Geomorphology* **207**: 213–220.

Karlén W. 1973. Holocene glacier and climatic variations, Kebnekaise mountains, Swedish Lapland. *Geografiska Annaler. Series A. Physical Geography* **55**(1): 29–63.

Kirkbride MP, Winkler S. 2012. Correlation of Late Quaternary moraines: impact of climate variability, glacier response, and chronological resolution. *Quaternary Science Reviews* **46**: 1–29.

Kjær KH, Larsen E, van der Meer J, Ingólfsson Ó, Krüger J, Benediktsson ÍÖ, Knudsen CG, Schomacker A. 2006. Subglacial decoupling at the sediment/bedrock interface: a new mechanism for rapid flowing ice. *Quaternary Science Reviews* **25**(21): 2704–2712.

Kleman J, Borgström I. 1996. Reconstruction of palaeo-ice sheets: the use of geomorphological data. *Earth Surface Processes and Landforms* **21**(10): 893–909.

Lukas S, Nicholson LI, Ross FH, Humlum O. 2005. Formation, meltout processes and landscape alteration of high-Arctic ice-cored moraines – examples from Nordenskiold Land, central Spitsbergen. *Polar Geography* **29**(3): 157–187.

Mattson LE, Gardner JS. 1991. Mass wasting on valley-side ice-cored moraines, Boundary Glacier, Alberta, Canada. *Geografiska Annaler. Series A. Physical Geography* **73**(3/4): 123–128.

Morris EM, Morland LW. 1976. A theoretical analysis of the formation of glacial flutes. *Journal of Glaciology* **17**: 311–323.

Orbring L. 2002. Front variations of isfallsglaciären during the 20th century, In Tarfala Research Station Annual Report 1999–2000 and 2000–2001, Klingbjer P (ed). Report no. 1. ISSN 1651–1506. 92 (70–71).

Paul MA, Evans H. 1974. Observations on the internal structure and origin of some flutes in glacio-fluvial sediments, Blomstrandbreen, north-west Spitsbergen. *Journal of Glaciology* **13**: 393–400.

Rabot C, Muret E. 1912. Les Variations périodiques des Glaciers XVIme Rapport. *Zeitschr. Gletscherkunde* **6**: 95–97 .*1911–1912*Leipzig

Rea BR, Evans DJ. 2011. An assessment of surge-induced crevassing and the formation of crevasse squeeze ridges. *Journal of Geophysical Research: Earth Surface* **116**: FO4005.

Rippin DM, Pomfret A, King N. 2015. High resolution mapping of supra-glacial drainage pathways reveals link between micro-channel drainage density, surface roughness and surface reflectance. *Earth Surface Processes and Landforms* **40**(10): 1279–1290.

Roberson S, Hubbard B, Coulson HR, Boomer I. 2011. Physical properties and formation of flutes at a polythermal valley glacier: Midre Lovénbreen, Svalbard. *Geografiska Annaler: Series A, Physical Geography* **93**(2): 71–88.

Rose J. 1991. Subaerial modification of glacier bedforms immediately following ice wastage. *Norsk Geografisk Tidsskrift* **45**(3): 143–153.

Ryan JC, Hubbard AL, Box JE, Todd J, Christoffersen P, Carr JR, Holt TO, Snooke N. 2015. UAV photogrammetry and structure from motion to assess calving dynamics at Store Glacier, a large outlet draining the Greenland ice sheet. *The Cryosphere* **9**(1): 1–11.

Schoof CG, Clarke GK. 2008. A model for spiral flows in basal ice and the formation of subglacial flutes based on a Reiner-Rivlin rheology for glacial ice. *Journal of Geophysical Research: Solid Earth* **113**: B05204.

Smith MJ, Clark CD. 2005. Methods for the visualization of digital elevation models for landform mapping. *Earth Surface Processes and Landforms* **30**(7): 885–900.

Smith MW, Carrivick JL, Quincey DJ. 2016. Structure from motion photogrammetry in physical geography. *Progress in Physical Geography* **40**(2): 247–275.

Spagnolo M, Clark CD, Hughes AL. 2012. Drumlin relief. *Geomorphology* **153**: 179–191.

Spagnolo M, Clark CD, Ely JC, Stokes CR, Anderson JB, Andreassen K, Graham AG, King EC. 2014. Size, shape and spatial arrangement of mega-scale glacial lineations from a large and diverse dataset. *Earth Surface Processes and Landforms* **39**(11): 1432–1448.

Stokes CR, Clark CD. 1999. Geomorphological criteria for identifying Pleistocene ice streams. *Annals of Glaciology* **28**(1): 67–74.

Stokes CR, Spagnolo M, Clark CD, Cofaigh CÓ, Lian OB, Dunstone RB. 2013. Formation of mega-scale glacial lineations on the Dubawnt Lake Ice Stream bed: 1. size, shape and spacing from a large remote sensing dataset. *Quaternary Science Reviews* **77**: 190–209.

Stokes CR, Tarasov L, Blomdin R, Cronin TM, Fisher TG, Gyllencreutz R, Hättestrand C, Heyman J, Hindmarsh RC, Hughes AL, Jakobsson M. 2015. On the reconstruction of palaeo-ice sheets: recent advances and future challenges. *Quaternary Science Reviews* **125**: 15–49.

Storrar RD, Stokes CR, Evans DJ. 2013. A map of large Canadian eskers from Landsat satellite imagery. *Journal of Maps* **9**(3): 456–473.

Storrar RD, Stokes CR, Evans DJ. 2014. Morphometry and pattern of a large sample (>20 000) of Canadian eskers and implications for subglacial drainage beneath ice sheets. *Quaternary Science Reviews* **105**: 1–25.

Storrar RD, Evans DJ, Stokes CR, Ewertowski M. 2015. Controls on the location, morphology and evolution of complex esker systems at decadal timescales, Breiðamerkurjökull, southeast Iceland. *Earth Surface Processes and Landforms* **40**(11): 1421–1438.

van der Meer JJ. 1997. Short-lived streamlined bedforms (annual small flutes) formed under clean ice, Turtmann Glacier, Switzerland. *Sedimentary Geology* **111**: 107–118.

Weertman J. 1957. On the sliding of glaciers. *Journal of Glaciology* **3**(21): 33–38.

WGMS FoG database version: 2015–11-25. http://www.wgms.ch/EsriDE/min-data-graphs/333_FV_cum.png last accessed 26/05/2016.

